JOURNAL OF PHYSICAL ORGANIC CHEMISTRY
J. Phys. Org. Chem. 2003; **16:** 700–708
Published online in Wiley InterScience (www.interscience.wiley.com). DOI: 10.1002/poc.684

Influence of solvent polarity on the stereoselectivity of the uncatalyzed [4 + 2] cycloaddition of cyclopentadiene to an *N,N′*-fumaroyl bis-(six-membered ring [(2*R*)-10a-homobornane-10a,2-sultam])

Anna Piątek,[1] Christian Chapuis[2†] and Janusz Jurczak[1,2]*

[1]Department of Chemistry, University of Warsaw, Pasteura 1, PL-02-093 Warsaw, Poland
[2]Institute of Organic Chemistry, Polish Academy of Sciences, Kasprzaka 44/52, PL-01-224 Warsaw, Poland

Received 19 December 2002; revised 24 May 2003; accepted 26 May 2003

ABSTRACT: A new six-membered ring (2*R*)-bornane-10a,2-sultam was tested as chiral auxiliary for the [4 + 2] cycloaddition of cyclopentadiene to the bis-fumaroyl derivative (–)-**1f** and shows under chelating conditions similar complete selectivity to Oppolzer's sultam. Inversion of the π-face selectivity is nevertheless observed under uncatalyzed conditions under the influence of solvent polarity, varying from 82% *de* for the (2*R*,3*R*) cycloadduct **2f** in trifluoroethanol to 70% *de* in favour of the (2*S*,3*S*) diastereoisomer in hexane as solvent. A predictive linear correlation is observed between the stereoselectivity and the solvent parameters according to the Abboud–Abraham–Kamlet-Taft model. PM3 calculations allowed a rationalization of these results based on the transition-state dipole moment. Illustrated by an x-ray analysis of cycloadduct (2*S*,3*S*)-**2f**, the main structural differences and influences in terms of steric and stereoelectronic factors are discussed by comparison of the five- versus six-membered ring homologues. Copyright © 2003 John Wiley & Sons, Ltd.

KEYWORDS: polarity; stereoselective; asymmetric; cycloaddition; Diels–Alder; sultam

INTRODUCTION

We recently presented the complete π-facial selectivity shown by the $TiCl_4$-catalyzed [4 + 2] cycloaddition of cyclopentadiene to *N*-fumaroyl mono-and bis[(2*R*)-bornane-10,2-sultam], (–)-**1a,b** (Scheme 1).[1,2] In addition to the influence of diverse Lewis acids, and applications to diverse dienes,[3] we also reported in detail the influence of the solvent polarity, ranging from apolar CO_2 supercritical fluid to ionic liquid.[4] We observed that, in contrast to other auxiliaries,[5] a strong influence and a clear correlation between increasing solvent polarity, according to the Reichardt $E_T(30)$ scale,[6] and increasing π-facial selectivity was found during the uncatalyzed cycloaddition of (–)-**1b** to cyclopentadiene.[4] More recently, a similar observation was reported for the 1,3-dipolar azomethine ylid cycloaddition to (–)-**1c**.[7] In contrast, a reverse solvent effect was observed during the 1,3-dipolar addition of a nitrile oxide to the *N*-acryloyl derivative (–)-**1d**, and we made the same observation during the thermal [4 + 2] cycloaddition of cyclopentadiene to dienophile (–)-**1e**.[9] We also recently reported the synthesis of a six-membered ring sultam (–)-**R^c-H**,[10] homologous to the (–)-(2*R*)-bornane-10,2-sultam auxiliary (–)-**R^a-H**,[11] and we now wish to present a third example where the π-facial selectivity is completely reversed depending on the solvent employed.

RESULTS

Crystalline dienophile (–)-**1f** was obtained in 74% yield after deprotonation of (–)-(2*R*)-10a-homobornane-10a,2-sultam, (–)-**R^c-H**, with NaH (1.1 mol equiv.) in THF and addition of fumaroyl chloride (1.5 mol equiv.). When (–)-**1f** was treated at −78 °C in CH_2Cl_2 with 1.0 mol equiv. of $TiCl_4$ and 4.0 mol equiv. of cyclopentadiene, the cycloadduct (2*R*,3*R*)-**2f** was obtained in quantitative yield and 99% *de* after 18 h. A similar selectivity was also obtained under catalytic conditions (0.5 mol equiv., 98% yield). Under chelating conditions, dienophile (–)-**1f** is thus fully comparable in efficiency with its five-membered ring analogue (–)-**1b**.[2] When the same reaction was repeated in the absence of Lewis acid, the conversion after 18 h was incomplete (4% yield) and the diastereoselectivity

**Correspondence to:* J. Jurczak, Department of Chemistry, University of Warsaw, Pasteura 1, PL-02-093 Warsaw, Poland.
E-mail: jjurczak@chem.uw.edu.pl
†Present address: Firmenich SA, Corporate R & D Division, P.O. Box 239, CH-1211 Geneva, Switzerland.
Contract/grant sponsor: National Committee for Scientific Research; *Contract/grant number:* PBZ 6.05/T09/1999.

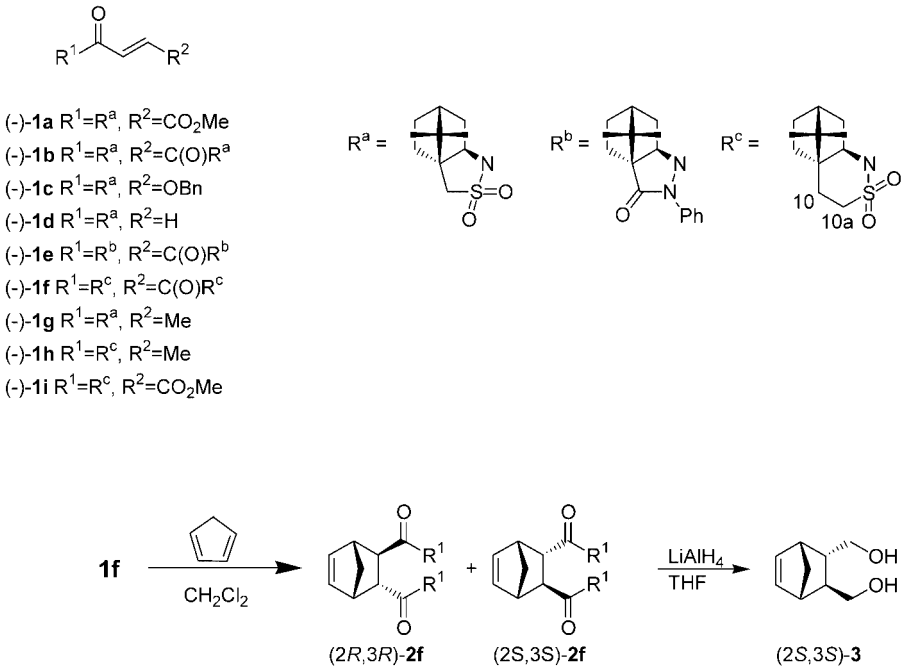

Scheme 1

dropped to 31% *de* in favour of the (2*R*,3*R*) diastereoisomer. When compared with the full conversion and 89% (2*R*,3*R*)-**2b** *de* obtained with (–)-**1b** under the same conditions,[2] we can conclude that (–)-**1f** is less reactive and selective under uncatalyzed conditions. This was confirmed when the reaction was performed at 20 °C since, after 18 h, the fully converted material exhibited 37% *de* in favor of (2*R*,3*R*)-**2f** as compared with 85% *de* in the case of (2*R*,3*R*)-**2b**.[2] The conversion and diastereoselectivity were readily measured directly by integration, in the 500 MHz ^{1}H NMR spectrum, of the olefinic signals of the crude diastereoisomeric mixture of cycloadducts **2f** with a precision of ±2% *de*. The stereoisomer (2*S*,3*S*)-**2f** shows signals at 6.16 and 6.22 ppm, while analogous signals for the second stereoisomer (2*R*,3*R*)-**2f** resonate at 5.95 and 6.38 ppm, as compared with the signal at 7.44 ppm for dienophile (–)-**1f**. The absolute configuration was determined by reduction of the stereoisomer (2*S*,3*S*)-**2f** to the known diol (–)-(2*S*,3*S*)-**3**[12] {$LiAlH_4$, 2.0 mol equiv. THF, 93% yield, SiO_2 hexane–Et_2O (7:3), $[\alpha]_D^{20} = -16.0$, $c = 1.1$, $CHCl_3$} with recuperation (94% yield) of the chiral auxiliary, and was independently confirmed by x-ray analysis of the crystalline cycloadduct (2*S*,3*S*)-**2f** as shown in Fig. 1.

By analogy with (–)-**1b**, we increased the solvent polarity, which resulted in an amelioration of the π-facial selectivity to 72% *de* in MeCN and 77% *de* in $MeNO_2$. As also earlier observed in the case of (–)-**1b**, the use of more polar but activating hydrogen bond donor protic solvents such as MeOH (45% *de*) or CF_3CH_2OH (82% *de*) (Table 1) resulted in a right-shifted parallel and similar polarity influence.[4] This certainly results from a different mechanistic/conformational pattern due to

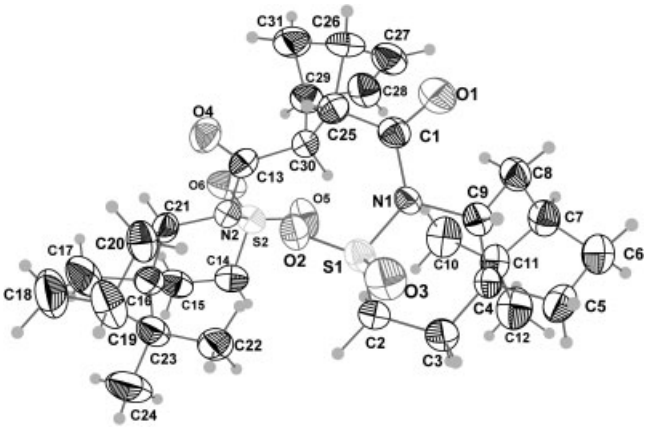

Figure 1. ORTEP diagram of (2*S*,3*S*)-**2f** with arbitrary atom numbering. Ellipsoids are represented at the 50% probability level

activation of the dienophile by H-bond complexation with the carbonyl moiety. When these two hydroxylic solvents are omitted, a good linear correlation ($r = 0.97$, $s = 0.154$) is obtained (see Fig. 2).

We then turned our attention to less polar solvents such as $CHCl_3$ (−12% *de*), AcOEt (−22% *de*) and toluene (−59% *de*) and observed inversion of the sense of π-facial selectivity, as reported earlier for another analogue of (–)-**1a**.[12] We thus could reach up to 70% *de* in favor of diastereoisomer (2*S*,3*S*)-**2f** in hexane by working under 0.0005 M high dilution conditions owing to the low solubility of dienophile (–)-**1f**, albeit with incomplete chemical conversion. Since the diastereoselectivity observed in the apolar Et_3N (−45% *de*) was not as high as expected, we then turned our attention towards a

Table 1. Dependence of the diastereoselectivity of the cycloaddition (–)-**1f** to **2f** on the polarity and solvatochromic indexes

Solvent	Conversion (%)	*de*	$E_T(30)$	Log(*dr*)	π^*	α	β	δ	Calculated	Residual
CF_3CH_2OH	100	82	59.8	1.005	0.73	1.51	0.00	0.0	0.983	0.022
MeOH	100	45	55.4	0.421	0.60	0.98	0.66	0.0	0.455	−0.034
$MeNO_2$	100	77	46.3	0.886	0.85	0.22	0.06	0.0	0.847	0.039
MeCN	100	72	45.6	0.788	0.76	0.00	0.29	0.0	0.577	0.211
CH_2Cl_2	100	37	40.7	0.337	0.82	0.13	0.10	0.5	0.335	0.002
$CHCl_3$	100	−12	39.1	−0.105	0.58	0.20	0.10	0.5	−0.060	−0.044
AcOEt	100	−22	38.1	−0.194	0.55	0.00	0.45	0.0	0.174	−0.369
Toluene	100	−59	33.9	−0.589	0.54	0.00	0.11	1.0	−0.610	0.021
Et_3N	100	−45	32.1	−0.421	0.14	0.00	0.71	0.0	−0.599	0.178
Hexane	16	−70	31.0	−0.753	−0.04	0.00	0.00	0.0	−0.727	−0.027

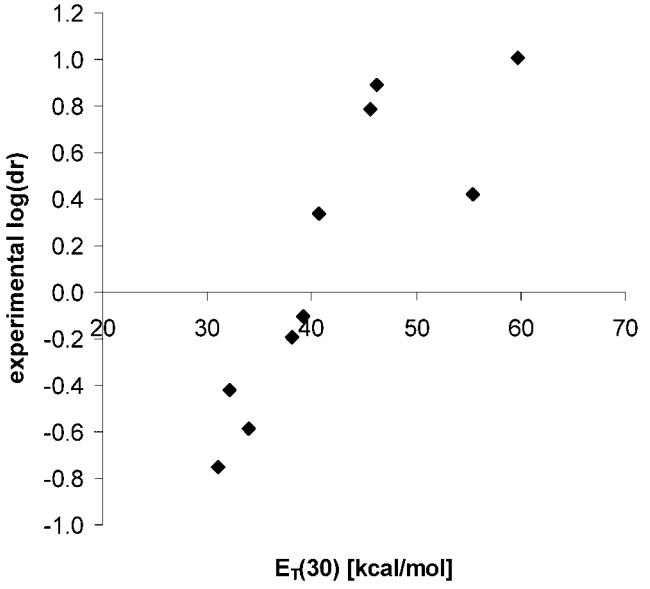

Figure 2. Diastereoselectivity of the uncatalyzed cycloaddition of (–)-**1f** to cyclopentadiene as a function of the solvent polarity as defined by the $E_T(30)$ values of Reichardt (*dr* = diastereoisomer ratio)

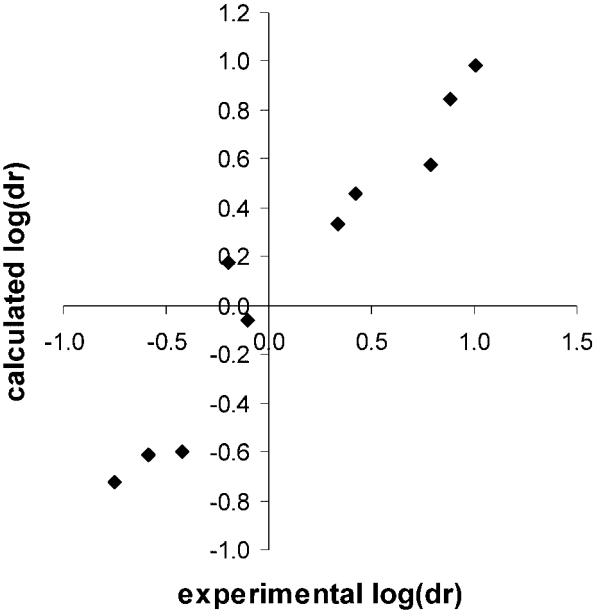

Figure 3. Experimental versus predicted diastereoselectivity of (–)-**1f** based on the Abboud–Abraham–Kamlet–Taft model (*dr* = diastereoisomer ratio)

more generalized definition of the polarity as expressed by the multi-parameter Abboud–Abraham–Kamlet–Taft model,[13] where log(*dr*) may by expressed as a linear correlation of diverse solvatochromic parameters as previously defined.[4] The π^*, α, β, δ and square of Hildebrand indexes are characteristic of the solvent and have been recently compiled Migron and Marcus[14] and Chastrette *et al.*[15] Based on 10 solvents, we found that the Hildebrand index as parameter of the cohesive pressure was statistically not relevant and could be omitted without further alteration of the linear correlation. Thus a good fit was found between the experimental and calculated diastereoselectivity [log(*dr*)] as shown in Fig. 3. A correlation coefficient of 0.97 was found ($r^2 = 0.94$) with a standard deviation of 0.21 when the equation was fitted with the following parameters:

$$\log(dr) = -0.658 + 1.723\pi^* - 0.854\delta + 0.253\alpha - 0.257\beta$$

Two additional solvatochromic parameters were nevertheless statistically not significant and a simpler correlation could be obtained with the π^* as well as δ solvatochromic parameters [$\log(dr) = -0.745 + 1.927\ \pi^* - 0.915\delta$; $r = 0.95$, $r^2 = 0.90$, $s = 0.237$] without significant loss of precision. Thus, 10 different experimental points are sufficient to evidence a linear correlation possessing two degrees of freedom and, since the solvent dependence is in line with our precedent results,[4,9,16] we decided that further examples would be unnecessary. The most divergent result was obtained in AcOEt.

DISCUSSION

For both s-*cis* and s-*trans* conformations, we calculated the energies of the rotamers around the N—C(O) bond of the simplified *N*-crotonoyl dienophile (–)-**1h**. When compared with the results reported for the analogous dienophile (–)-**1g** (see Fig. 4),[16] one notices remarkable

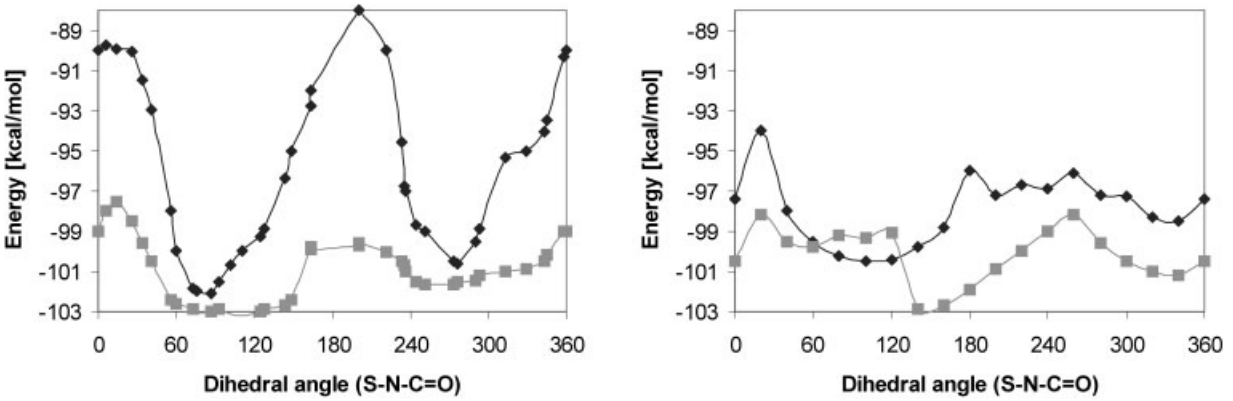

Figure 4. Rotamer energies for s-*cis* (□) and s-*trans* (■) (–)-**1h** (left) and (–)-**1g** (right)

differences. Thus, for example, the practically coplanar conformations (ca 160 and 340 °) are no longer among the lowest energy conformations. In the case of the six-membered ring analogue (–)-**1h**, the most stable conformations are around 90 and 270 ° and these orthogonal conformations are energetically very close to each other with respect to both s-*cis* and s-*trans* conformers. Furthermore, these energetic wells are much wider in comparison with those reported for (–)-**1g**, ranging from ca 60 to 140 ° and 240 to 330 °.

In order to monitor whether a more bulky substituent in the β-position could modify the energetic profile of the rotamers around the N—C(O) bond, we systematically performed the same calculations for the s-*cis/trans*-s-*cis* and s-*cis/trans*-s-*trans* coplanar conformations of the *N*-fumaroyl derivatives (–)-**1a** and (–)-**1i**. The results reported in Figs 5 and 6 show that very similar behavior and identical conclusions arise from the comparison of the five- versus six-membered ring analogues. In the case of (–)-**1a**, the π-system of the dienophile may easily profit from the conjugation with the sultam moiety (ca 160 and 340 °) with a remarkable differentiated energy in favor of the s-*cis*-s-*cis/trans* as compared with the s-*trans*-s-*cis/trans* conformers. In contrast, the six-membered ring

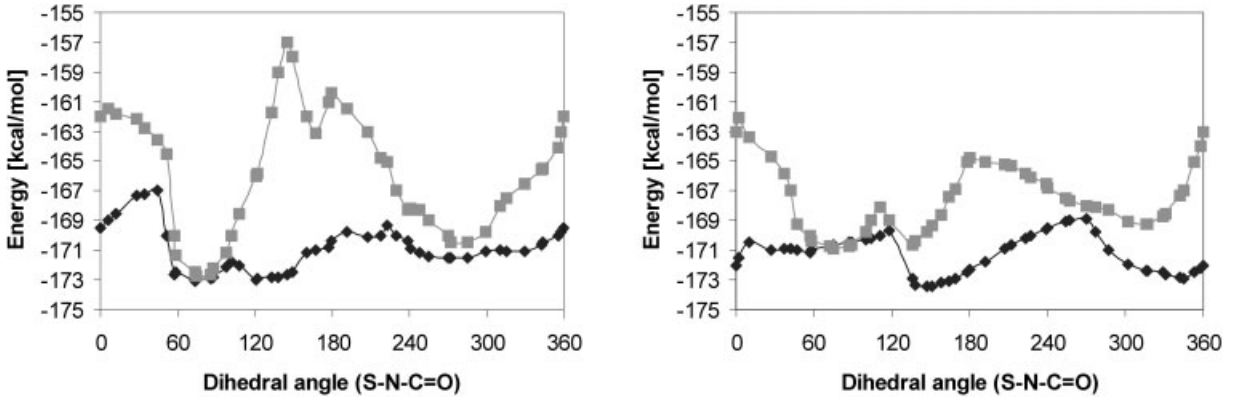

Figure 5. Rotamer energies for s-*cis*-s-*cis* (■) and s-*trans*-s-*cis* (□) (–)-**1i** (left) and (–)-**1a** (right)

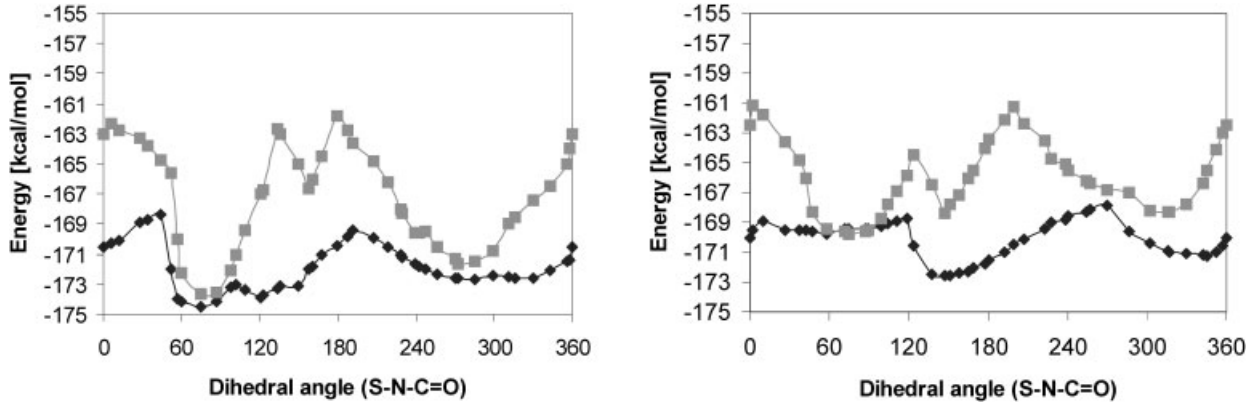

Figure 6. Rotamer energies for s-*cis*-s-*trans* (■) and s-*trans*-s-*trans* (□) (–)-**1i** (left) and (–)-**1a** (right)

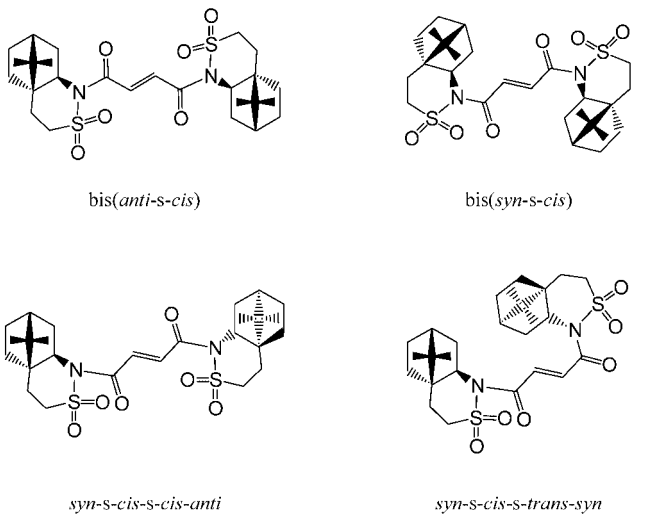

Scheme 2

analogous dienophile (–)-**1i** imposes orthogonal conformations (ca 80 and 270°) with very poor energetic differentiations between s-*cis* and s-*trans* conformations of the $C_\alpha{=}C_\beta$ double bond.

Based on semi-empirical PM3 calculations,[17] we earlier rationalized the increasing diastereoselectivity observed in polar solvents during the uncatalyzed cycloaddition of cyclopentadiene to (–)-**1b** by the fact that the transition states resulting from the Cα-*re* attack possessed systematically a higher dipole moment compared with the energetically disfavored corresponding Cα-*si* face transition states.[4] Alternatively, the situation was inverted in the case of dienophile (–)-**1e**.[9] Using the same method of calculation and constraining parameters (0.05 mdyn Å^{-2} for S—N—C=O and 0.2 mdyn Å^{-2} for the O=C—C=C torsional angles),[18] we systematically determined the energies of the transition states for all possible coplanar and orthogonal conformers of (–)-**1f** (four of them are shown in Scheme 2). For each nonsymmetric conformer, both pseudo '*endo*' and '*exo*' approaches were calculated for both faces, but only the lowest energy is reported in Table 2.

Furthermore, only the five most stable coplanar conformers are disclosed, since the conformational energies and the transition-state energies of the others are far larger and thus do not statistically intervene in the stereoselective course of this reaction. Thus, for example, in these undisclosed series, the conformational energy varies from −186.82 kcal mol^{-1} for the *bis*(*syn*-s-*trans*) conformer to −193.95 kcal mol^{-1} for the *syn*-s-*cis*-s-*trans*-*anti* conformer (1 kcal = 4.184 kJ). The lowest unreported transition state was obtained for the Cα-*re* face attack on the latter, with an energy of −128.85 kcal mol^{-1}.

In order to determine if the lowest diastereoselectivity observed for (–)-**1f** as compared with (–)-**1b** results from this higher flexibility and from the smaller s-*cis*/s-*trans* conformational energetic differences, we also systematically calculated the energies for the

Table 2. PM3-calculated conformational energies, LUMO, Cα atomic coefficients and transition state $\Delta H^\ddagger$ and dipole moment **1f**

Conformer	ΔH_{form} (kcal mol^{-1})	LUMO (eV)	TS‡ S—N—C=O[a] (°)	TS‡ S′—N′—C′=O′ (°)	Cα-*re* face attack Cα-*re*	Cα′-*re*	$\Delta H^\ddagger re$ (kcal mol^{-1})	Dipolemoment (D)	Cα-*si* face attack Cα-*si*	Cα′-*si*	$\Delta H^\ddagger si$ (kcal mol^{-1})	Dipolemoment (D)
syn-s-*cis*-s-*cis*-*anti*	−196.72	−0.86	−24.8	142.4	−0.12	0.14	−131.69	7.9	0.15	−0.15	−129.43	6.5
Bis(90-s-*trans*)	−197.35	−1.02	81.7	89.0	−0.22	0.22	−128.13	8.3	0.21	−0.24	−125.51	5.6
Bis(*anti*-s-*cis*)	−197.45	−1.06	145.4	126.5	−0.13	0.15	**−134.57**	**7.2**	0.17	−0.16	−126.82	4.7
90-s-*trans*-s-*trans*-270	−197.68	−1.03	101.5	273.3	−0.21	0.24	−125.38	4.26	0.25	−0.24	−127.22	5.1
Bis(*syn*-s-*cis*)	−197.83	−1.03	−24.3	52.4	−0.25	0.24	−130.63	2.6	0.24	−0.24	−128.21	0.8
90-s-*cis*-s-*cis*-270	−197.93	−1.08	112.1/115.1	290.8/283.9	−0.23	0.21	*−132.93*	*4.6*	0.21	−0.21	*−133.6*	*5.8*
90-s-*trans*-s-*cis*-270	−198.07	−1.06	71.6	264.9	−0.26	0.25	−131.67	8.8	0.22	−0.21	−127.97	10.0
Bis(90-s-*cis*)	−198.27	−1.15	115.3/76.6	114.6/62.4	−0.24	0.21	**−134.40**	**7.6**	0.23	−0.23	*−134.22*	*4.6*
90-s-*cis*-s-*trans*-270	−198.82	−1.12	92.3	285.2	−0.23	0.22	−128.81	11.5	0.26	−0.22	**−134.94**	**7.9**
syn-s-*trans*-s-*cis*-*anti*	−198.93	−1.00	68.2	120.8	−0.19	0.21	−129.59	7.9	0.21	−0.21	−131.93	6.8
syn-s-*cis*-s-*trans*-*syn*	−200.07	−1.03	−26.1	63.8	−0.25	0.22	−128.54	11.4	0.25	−0.23	−130.58	10.7
90-s-*cis*-s-*trans*-90	−200.23	−1.05	94	114.6	−0.21	0.20	−131.50	6.2	0.22	−0.24	−129.95	8.4

[a] Angles of the lowest transition state.

orthogonal conformers. We found five conformers below $-196.5\,kcal\,mol^{-1}$, the most stable one being the 90-s-*cis*-s-*trans*-90 conformation with $-200.23\,kcal\,mol^{-1}$. Nevertheless, the transition states derived from this latter conformation are fairly high in energy when compared with the lowest one (see Table 2). With an energy of $-193.44\,kcal\,mol^{-1}$ the bis(270-s-*trans*) conformer does not statistically influence the reaction, while the transition states of both other orthogonal bis-s-*trans* conformers are too high in energy. The minimum at $-134.94\,kcal\,mol^{-1}$ is reached for the Cα-*si* attack on the 90-s-*cis*-s-*trans*-270 conformer. Alternatively, taking into account the heat of formation of 1,3-cyclopentadiene at infinite separation ($31.75\,kcal\,mol^{-1}$), the lowest barrier is found between the bis(*anti*-s-*cis*) conformer and its Cα-*re* transition state at $-134.57\,kcal\,mol^{-1}$.

We indicate in bold and italics the most relevant transition states within $3.0\,kcal\,mol^{-1}$ of the lowest one. The transition states having a large dipole moment are indicated in bold, and those in italics refer to a smaller dipole moment. Consequently, in very polar solvents, one Cα-*si* attack on the 90-s-*cis*-s-*trans*-270 conformer resulting in a transition-state barrier of $32.13\,kcal\,mol^{-1}$ competes with two kinetically favoured Cα-*re* attacks on the bis(*anti*-s-*cis*) and bis(90-s-*cis*) symmetric conformers with transition barriers of 31.13 and $32.12\,kcal\,mol^{-1}$, respectively. This rationalizes the higher selectivity for the (2*R*,3*R*)-cycloadduct **2f** in polar solvents. Under apolar conditions, the highly polar transition states are disfavoured and their overall participation diminishes. Thus, in particularly apolar solvents two Cα-*si* attacks on the bis(90-s-*cis*) and 90-s-*cis*-s-*cis*-270 conformers with transition barriers of 32.30 and $32.56\,kcal\,mol^{-1}$, respectively, compete with a single less favorable Cα-*re* attack ($33.24\,kcal\,mol^{-1}$) on the latter conformer, thus favouring the (2*S*,3*S*)-cycloadduct **2f**. Between these two theoretical extremes, the stereochemical course of the reaction is determined by a combination of these six transition states depending on the solvent polarity.

Amongst the reactive coplanar conformations presented here, two of them orientate the N lone pairs in opposite directions, while the *syn*-s-*trans*-s-*cis*-*anti* and both symmetric bis(*syn*-s-*cis*) and bis(*anti*-s-*cis*) conformers orientate their N lp in a cumulative unidirectional way. Nevertheless, as expressed by the atomic coefficients on the Cα-*re* and *si* faces (see Table 2), this stereoelectronic influence is small and the π-face opposite to the N lp is only slightly privileged to an insignificant extent from an electronic point of view. This weak stereoelectronic influence is further confirmed when the steric interactions are also considered. Indeed, the privileged Cα-*re* attack on the bis(*anti*-s-*cis*) conformer corresponds to a mismatching steric and stereoelectronic interactions, while the bis(*syn*-s-*cis*) conformer which cooperatively cumulates both steric and stereoelectronic factors[18] does not even participate in the overall stereochemical course of this cycloaddition. These features are thus in complete contrast with those imposed on dienophile (–)-**1b** by the analogous five-membered ring sultam (–)-**R^a-H**.

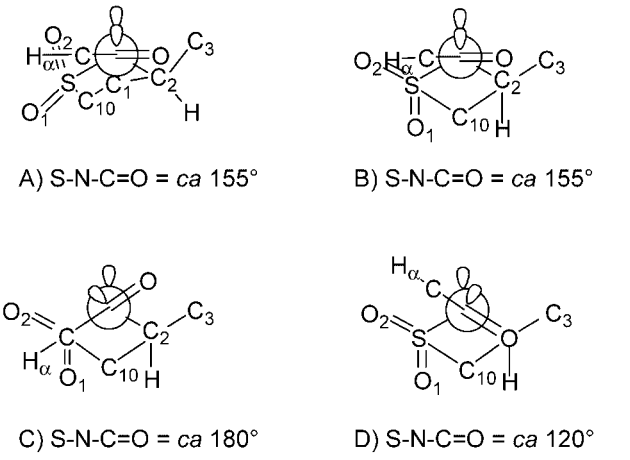

Figure 7. Newman projections of the S—N—C═O portion of the five- and six-membered ring sultams

This may by rationalized by inspection of the Newman projection of the S—N—C═O portion (Fig. 7). In the case of the five-membered ring, the thermodynamically stable, practically coplanar conformation (projection A) allows a perfect alignment of the dienophilic π-system with the N lp and fully profits from delocalization with the electron-withdrawing sultam moiety. The Cα—H substituent practically bisects the O(1)═S═O(2) moiety in this *anti*-s-*cis* example. Since the same argument may be used for the *syn*-s-*cis* conformation with the pseudo-equatorial C(3), we shall therefore discuss only one conformation. In the case of the six-membered ring, the alignment of the π-system is precluded by the severe steric interactions of both Cα-H/S═O(2) and C═O/C(3), due to the equatorial orientation of these substituents (projection B). The stereoelectronic alignment is thus lost and furthermore a destabilizing steric interaction between the C═O and C(3)H_2 is observed when the S—N—C═O angle reaches ca 180° (projection C). The single steric interaction between the Cα—H/S═O(2) is less destabilizing when the S—N—C═O torsional angle is about 120° (projection D). Although the lowest energy conformations are reached when the angle is about 70–90° (see Table 2 and Fig. 3), a second low-energy region occurs at 265–285° but is slightly higher in energy.

The x-ray analysis of (2*S*,3*S*)-**2f** (Fig. 1, Table 3) clearly shows one S—N—C═O dihedral angle at ca 120° and the second at 137° as expected from PM3 conformational analysis (Fig. 3) and transition-state calculations (Table 2). Following the usual trends of sultams, but in contrast to (–)-**R^a-H**,[10] the S—N bond is shorter than the S—C bond while the N lp is antiperiplanar to the axial S═O(1) substituent. The N atoms in cycloadduct (2*S*,3*S*)-**2f** are more pyramidalized than that exhibited by the x-ray analysis of the free (–)-**R^c-H**[10] and

Table 3. Selected bond lengths (Å) and angles (°) of (2*S*,3*S*)-**2f**

Bond or angle	Parameter	Value	Parameter	Value
S═O	S1═O2	1.430(4)	S2═O5	1.420(5)
S═O	S1═O3	1.429(4)	S2═O6	1.434(5)
S—N	S1—N1	1.659(4)	S2—N2	1.667(5)
S—C	S1—C2	1.774(7)	S2—C14	1.751(7)
N—C	N1—C9	1.503(7)	N2—C21	1.513(7)
N—C(O)	N1—C1	1.458(8)	N2—C13	1.449(8)
O═S═O	O2═S1═O3	117.6(2)	O5═S2═O6	118.1(3)
C—N—S	C9—N1—S1	112.2(4)	C21—N2—S2	115.2(4)
C—N—C(O)	C9—N1—C1	116.3(4)	C21—N2—C13	112.3(5)
S—N—C(O)	S1—N1—C1	117.1(4)	S2—N2—C13	117.2(4)
C—N—S═O	C9—N1—S1═O2	178.4(4)	C21—N2—S2═O5	−166.2(5)
C—N—S═O	C9—N1—S1═O3	49.1(4)	C21—N2—S2═O6	63.4(5)
C—C—N—S	C8—C9—N1—S1	173.3(5)	C20—C21—N2—S2	162.4(5)
C(O)—N—S═O	C1—N1—S1═O2	40.1(5)	C13—N2—S2—O5	58.2(5)
S—N—C═O	S1—N1—C1═O1	121.3(5)	S2—N2—C13—O4	137.1(5)
Δ*h*N		0.352(5)		0.340(4)

consequently the S—N bonds are slightly longer. The axial S═O(1) bond lengths are also equal to or longer than those of the corresponding equatorial S═O(2) moieties.

Five of the six lowest energy transition states under consideration originate from the bis(s-*cis*) conformers. Finally, keeping this part of the π-system rigid, we systematically fully rotated, in increments of 30°, both extreme SO_2N—C(O) torsion angles for the Cα-*re* attack. None of these generated transition states were lower in energy than those already calculated for both coplanar and orthogonal angles. On the same face and for the rigidified s-*cis*-s-*trans* conformation, systematic rotation of both prosthetic groups in 30° increments did not allow us to find a transition state lower than $-134.57\ \text{kcal mol}^{-1}$, thus confirming the kinetic origin of the (2*R*,3*R*) stereoselectivity when using polar solvents.

CONCLUSION

Under Lewis acid-mediated chelating conditions, dienophile (–)-**1f** derived from the six-membered ring sultam (–)-**R^c-H** behaves efficiently and similarly to its five-membered ring analogue (–)-**1b** with up to 99% *de* in favour of the (2*R*,3*R*) cycloadduct (–)-**2f**. Addition of a single methylene link in the five-membered ring sultam moiety of dienophile (–)-**1b** results in important, unfavourable changes in the chemical reactivity and stereoselectivity under uncatalyzed conditions. This originates from the conformational non-alignment of the dienophilic reactive π-system with the N lp of the prosthetic group due to the geometry of the six-membered ring. By modification of the solvent polarity, we could nevertheless reach, in trifluoroethanol, up to 82% *de* in favour of the (2*R*,3*R*) cycloadduct **2f** and, conversely, up to 70% *de* in favor of the (2*S*,3*S*) adduct **2f** in hexane. The dienophiles derived from (–)-**R^c-H** such as (–)-**1f**,**h** are also characterized by greater rotational barriers but increased number of possible rotamers around the S—N—C═O bond, in addition to their propensity to adopt orthogonal and s-*trans* conformations when compared with their conformationally, particularly rigidified five-membered ring analogues (–)-**1b**,**g**.

PM3 calculations allowed us to find three low-energy transition states exhibiting a high dipole moment and three other less polar ones, allowing a rationalization of the observed inversion of stereoselectivity dependent on the solvent polarity. Although our rationalization fits the observed experimental data well, we cannot exclude that conformers of the —SO_2N—C(O)—CH═CH—C(O)—NSO_2— π-system other than coplanar and orthogonal geometries may participate in the overall stereochemical course of this reaction, since only the specific thermodynamically favoured bis(s-*cis*) and s-*cis*-s-*trans* conformations were systematically calculated with a rotational increment of 30° for the Cα-*re* face.

EXPERIMENTAL

General.[19] Crystal data regarding structure (2*S*,3*S*)-**2f** are given in Table 4. All measurements of crystals were performed on a Kuma KM4CCD k-axis diffractometer with graphite-monochromated Mo Kα radiation. The crystal was positioned at 65 mm from the KM4CCD camera; 288 frames were measured at 1.6° intervals with a counting time of 10 s. The data were corrected for Lorentz and polarization effects. An Na absorption correction was applied. Data reduction and analysis were carried out with the Kuma Diffraction (Wrocław) programs.

The structure was solved by direct methods[20] and refined using SHELXL.[21] The refinement was based on F^2 for all reflections except those with very negative F^2. Weighted *R* factors *wR* and goodness-of-fit *S* values are based on F^2. Conventional *R* factors are based on *F* with

Table 4. Crystal data and structure refinement of (2*S*,3*S*)-**2f**

Empirical formula	$C_{32}H_{45}Cl_3N_2O_6S_2$		
Formula weight	724.17		
Temperature (K)	293(2)		
Wavelength (Å)	0.71073		
Crystal system	Monoclinic		
Space group	$P2_1$		
Unit cell dimensions			
(Å)	$a = 14.013(3)$, $b = 9.0085(18)$, c = 15.179(3)		
(°)	$\alpha = 90$, $\beta = 116.01(3)$, $\gamma = 90$		
Volume (Å^3)	1722.1(6)		
Z	2		
Density (Mg m^{-3})	1.397		
Absorption coefficient (mm^{-1})	0.433		
F(000) electrons	764		
Crystal size (mm)	0.53	0.44	0.18
T range for data (°)	3.48	22.00	
Index ranges	$-14 \leq h \leq 14$	$-9 \leq k \leq 9$	$-15 \leq l \leq 15$
Reflections collected	21312	4203	
R(int)	0.0696		
Refinement method	Full-matrix least-squares of F^2		
Data/restraints/parameters	4203/1/586		
Goodness-of-fit on $F2$	1.066		
Final R indices [$I > 2\sigma(I)$]	$R_1 = 0.0560$, $wR_2 = 0.1244$		
R indices (all data)	$R_1 = 0.0638$, $wR_2 = 0.1310$		
Abs. struct. parameter	−0.17		
Extinction coefficient	0.0057(13)		
Largest peak and holes (e Å^{-3})	0.360	−0.295	

F set to zero for negative F^2. The $F_0^2 > 2\sigma(F_0^2)$ criterion was used only for calculating R factors and is not relevant to the choice of reflection for the refinement. The R factors based on F^2 are about twice as large as those based on F. All hydrogen atoms were located from a differential map and refined isotropically. Scattering factors were taken from Tables 6.1.1.4 and 4.2.4.2 in Ref. 22. The known configuration of the asymmetric centres of the sultam unit was confirmed by the Flack-parameter refinement.[23] Crystallographic data (excluding structural factors) for the structure (2*S*,3*S*)-**2f** have been deposited as supplementary material with the Cambridge Crystallographic Data Centre and allocated the deposition number CCDC 184595.

Dienophile (−)-**1f**. A solution of the six-membered ring (2*R*)-10a-homobornane-10a,2-sultam[10] (500 mg, 2.2 mmol) in toluene (10 ml) was added to a suspension of NaH (250 mg, 6.1 mmol, 2.5 mol equiv.) in toluene (25 ml). After 30 min at 20 °C, a solution of freshly distilled fumaroyl chloride (0.13 ml, 1.2 mmol, 0.5 mol equiv.) in toluene (5 ml) was added. After 18 h at 20 °C, the mixture was heated at 40 °C for 1.5 h and 15% aqueous $NaHCO_3$ was added to the cold solution. After separation, the aqueous phase was extracted (3 × 10 ml) with CH_2Cl_2 and the organic phase was dried ($MgSO_4$) and concentrated under vacuum. The residue was purified by column chromatography [SiO_2, hexane–AcOEt (8:2)] to furnish pure dienophile (−)-**1f** in 74% yield, m.p. 220–222 °C (hexane–AcOEt). $[\alpha]_D^{20} = -22.1$ ($c = 1.0$, $CHCl_3$); $R_f = 0.14$ [hexane–AcOEt (3:2)]. IR (KBr): 3437, 2957, 1679, 1340, 1285.5, 1180, 763. ^{1}H NMR: 0.95 (s, 6H); 1.20 (s, 6H), 1.22 (m, 2H), 1.32 (m, 2H), 1.69 (m, 8H), 2.12 (dd, $J = 3.2$, 5.4 Hz, 2H), 2.18 (t, $J = 1.4$ Hz, 1H), 2.21 (t, $J = 6$ Hz, 1H), 2.33 (td, $J = 1.8$ Hz, 6, 2H), 3.11 (t, $J = 1.4$ Hz, 1H), 3.14 (t, $J = 1.6$ Hz, 1H), 4.42 (td, $J = 1.6$, 5.6 Hz, 2H); 3.96 (dAB, $J = 2.6$, 5.7 Hz, 2H); 7.44 (s, 2H). ^{13}C NMR: 20.3, 22.1, 24.3, 26.5, 36.3, 39.3, 45.9, 46.4, 47.9, 48.0, 66.6, 135.7, 166.2. HRMS: 561.2053; calculated for $C_{26}H_{38}N_2O_6NaS_2$ $[M + Na]^+$ 561.2064.

(−)-Cycloadduct (2R,3R)-**2f**. General procedure for the uncatalyzed cycloaddition: to a solution of (−)-**1f** (52 mg, 0.1 mmol) in the appropriate solvent (5 ml), cyclopentadiene (33 µl, 0.4 mmol) was added dropwise (along the cold wall of the reaction flask when not performed at 20 °C). After 18 h, the solvent and the excess of cyclopentadiene were evaporated under medium, then high vacuum. The crude cycloadduct **2f** (99% yield) was submitted to ^{1}H NMR analysis for *de* determination. M.p. 140–142 °C (hexane–AcOEt). $[\alpha]_D^{20} = -61.6$ ($c = 1.0$ $CHCl_3$); $R_f = 0.35$ [hexane–AcOEt (3:2)]. IR (film): 2958, 1704, 1340, 1158, 757. ^{1}H NMR: 0.64 (s, 6H), 1.18 (m, 2H), 1.24 (s, 3H), 1.27 (s, 3H), 1.41 (m, 2H), 1.51 (m, 1H), 1.67 (m, 9H), 2.05 (m, 1H), 2.16 (m, 3H), 2.29 (m, 2H), 3.14 (m, 3H), 3.44 (m, 3H), 3.85 (m, 1H), 3.9 (m, 2H), 4.63 (t, $J = 1.6$ Hz, 1H), 5.95 (dd, $J = 1.0$, 2.2 Hz, 1H), 6.38 (dd, $J = 1.2$, 2.2 Hz, 1H). ^{13}C NMR: 20.3, 20.35, 22.0, 22.2, 24.0, 24.02, 26.6,

26.7, 36.47, 36.5, 40.0, 40.4, 45.98, 46.0, 46.8, 46.84, 47.2, 47.6, 47.89, 47.91, 48.3, 49.7, 52.0, 52.05, 52.06, 66.6, 66.7, 133.6, 138.6, 174.95, 176.0. HRMS: 627.2542; calculated for $C_{31}H_{44}N_2O_6NaS_2$ $[M+Na]^+$ 627.2533.

(+)-Cycloadduct (2S,3S)-**2f**. Both diastereoisomeric cycloadducts could be separated by column chromatography [SiO_2, hexane–AcOEt (8:2) for analytical purposes. M.p. 212–216 °C (hexane–AcOEt). $[\alpha]_D^{20} = +109.2$($c = 1.0$, $CHCl_3$); $R_f = 0.38$ [hexane–AcOEt (3:2)]. IR (KBr): 2938, 1696, 1339, 1159, 719. ^{1}H NMR: 0.91 (s, 3H), 0.95 (s, 3H), 1.14 (s, 3H), 1.26 (s, 3H), 1.20–1.38 (m, 4H), 1.66 (m, 9H), 2.10 (m, 9H), 2.88 (dt, $J = 4$ Hz, 1H), 3.10 (dt, $J = 3.8$ Hz, 1H), 3.38 (m, 4H), 3.88 (m, 2H), 6.20 (m, 2H). ^{13}C NMR: 20.27, 20.3, 22.3, 22.7, 24.3, 24.5, 26.6, 26.7, 36.3, 36.7, 38.7, 39.6, 42.7, 44.7, 45.8, 46.2, 47.0, 47.6, 47.9, 48.6, 49.1, 52.9, 56.7, 61.2, 61.35, 66.8, 67.55, 136.8, 138.2, 174.9, 176.0. HRMS: 627.2514; calculated for $C_{31}H_{44}N_2O_6NaS_2$ $[M+Na]^+$ 627.2533.

Acknowledgements

The x-ray analysis of (2*S*,3*S*)-**2f** was recorded by the crystallographic department of the University of Warsaw. Financial support from the National Committee for Scientific Research (PBZ 6.05/T09/1999) is gratefully acknowledged.

REFERENCES

1. Chapuis C, Rzepecki P, Bauer T, Jurczak J. *Helv. Chim. Acta* 1995; **78**: 145–150.
2. Achmatowicz M, Chapuis C, Rzepecki P, Jurczak J. *Helv. Chim. Acta* 1999; **82**: 182–190.
3. Bauer T, Chapuis C, Kucharska A, Rzepecki P, Jurczak J. *Helv. Chim. Acta* 1998; **81**: 324–329.
4. Chapuis C, Kucharska A, Rzepecki P, Jurczak J. *Helv. Chim. Acta* 1998; **81**: 2314–2325.
5. Sauer J, Kredel J, *Tetrahedron Lett.* 1966; 6359–6364; Poll T, Helmchen G, Bauer B. *Tetrahedron Lett.* 1984; **25**: 2191–2194; Cativiela C, Garcia JI, Mayoral JA, Royo AJ, Salvatella L. *Tetrahedron: Asymmetry* 1993; **4**: 1613–1618; Saito F, Kawamura M, Nishimura JI. *Tetrahedron Lett.* 1997; **38**: 3231–3234; Naraku G, Hori K, Ito YN, Katsuki T. *Tetrahedron Lett.* 1997; **38**: 8231–8232; Cativiela C, Garcia JI, Gil J, Martinez RM, Mayoral JA, Salvatella L, Urieta JS, Mainar AM, Abraham MH. *J. Chem. Soc., Perkin Trans. 2* 1997; 653–660; Otto S, Boccaletti G, Engberts JBFN. *J. Am. Chem. Soc.* 1998; **120**: 4238–4239.
6. Reichardt C. *Solvent Effects in Organic Chemistry.* Verlag Chemie: Weinheim, 1979; Reichardt C. *Chem. Rev.* 1994; **94**: 2319–2358; Reichardt C, Schäfer G. *Liebigs Ann.* 1995; 1579–1582; Eberhardt R, Löbbecke S, Neidhart B, Reichardt C. *Liebigs Ann./Recl.* 1997; 1195–1199.
7. Karlsson S, Högberg HE. *Tetrahedron: Asymmetry* 2001; **12**: 1977–1982.
8. Curran DP, Kim BH, Daugherty J, Heffner TA. *Tetrahedron Lett.* 1988; **29**: 3555–3558.
9. Chapuis C, Kucharska A, Jurczak J. *Tetrahedron: Asymmetry* 2000; **11**: 4581–4591.
10. Piatek A, Chapuis C, Jurczak J. *Helv. Chim. Acta* 2002; **85**: 1973–1988.
11. Oppolzer W, Chapuis C, Bernardinelli G. *Helv. Chim. Acta* 1984; **67**: 1397–1401.
12. Horton D, Machinami T. *J. Chem. Soc., Chem. Commun.* 1981; 88–90; Horton D, Machinami T, Takagi Y. *Carbohydr. Res.* 1983; **121**: 135–161; Takano S, Kurotaki A, Ogasawara K. *Synthesis* 1987; 1075–1078; Saito S, Hama H, Matsuura Y. Okada K, Moriwake T. *Synlett*. 1991; 819–820.
13. Kamlet MJ, Abboud JL, Abraham MH, Taft RW. *J. Org. Chem.* 1983; **48**: 2877–2887.
14. Migron Y, Markus Y. *J. Chem. Soc., Faraday Trans.* 1991; **87**: 1339–1343.
15. Chastrette M, Rajzmann M, Chanon M, Purcell KF. *J. Am. Chem. Soc.* 1985; **107**: 1–11.
16. Chapuis C, Kawecki R, Urbanczyk-Lipkowska Z. *Helv. Chim. Acta* 2001; **84**: 579–588.
17. Stewart JJP. *J. Comput.-Aided Mol. Des.* 1990; **4**: 1–105.
18. Chapuis C, de Saint Laumer JY, Marty M. *Helv. Chim. Acta* 1997; **80**: 146–172.
19. Raczko J, Achmatowicz M, Jezewski A, Chapuis C, Urbanczyk-Lipkowska Z, Jurczak J. *Helv. Chim. Acta* 1998; **81**: 1264–1277.
20. Sheldrick GM. *Acta Crystallogr., Sect. A* 1990; **46**: 467–473.
21. Sheldrick GM. *SHELXL93. Program for Refinement of Crystal Structure*. University of Göttingen: Göttingen, 1993.
22. Wilson AJC (ed). *International Tables for Crystallography*, vol. C. Kluwer: Dordrecht, 1992.
23. Flack HD, Bernardinelli G. *Acta Crystallogr., Sect. A* 1999; **55**: 908–915; Flack HD, Bernardinelli G. *J. Appl. Crystallogr.* 2000; **33**: 1143–1148.